^{1}H NMR Study of the Electronic and Molecular Structure of the Heme Cavity in Horseradish Peroxidase. Complete Heme Resonance Assignments Based on Saturation Transfer and Nuclear Overhauser Effects

V. Thanabal,[1a] Jeffrey S. de Ropp,[1b] and Gerd N. La Mar*[1a]

Contribution from the Department of Chemistry and UCD NMR Facility, University of California, Davis, California 95616. *Received June 20, 1986*

Abstract: ^{1}H NMR saturation transfer spectroscopy and nuclear Overhauser effect, NOE, measurements have been utilized in conjunction with previous isotope labeling to effect a comprehensive assignment of the heme resonances in the low-spin cyano complex of horseradish peroxidase, HRP. The three methods permit for the first time location and identification of all 22 heme substituent resonances, including 12 resonances which are not resolved outside the intense diamagnetic envelope. Saturation transfer between resting-state HRP and its cyano complex, HRPCN, is modulated by a rapid CN^- off-rate ($\sim$2.5 s^{-1} at 55 °C) and allows detection of all resonances in HRPCN which had previously been assigned in resting-state HRP. NOE measurements as a function of saturation time reveal only primary NOEs for saturation times of <50 ms; spin-diffusion is clearly detected for saturation times > 100 ms. Of the three methods utilized, NOEs have the widest scope and applicability in paramagnetic proteins, particularly when used in conjunction with limited selective isotope labeling. Time-dependent NOE measurement on a propionate methylene pair yields a correlation time of 20 ns at 55 °C, which is consistent with the overall protein tumbling time. This indicates that the propionate is immobile in the heme pocket. NOEs between pairs of heme substituents demonstrate that the 2-vinyl and 4-vinyl groups are close to coplanar with the heme and possess trans and cis orientations, respectively. The pattern of the dominant dipolar shifts of the assigned meso-H resonance allows us to locate the in-plane magnetic axes as coincident with the N-Fe-N vectors of the heme. The pattern of the asymmetric heme methyl contact shifts locates the lone unpaired spin primarily in d_{yz}, which in turn determines the sign of the rhombic magnetic anisotropy. The detailed definition of the magnetic properties of the heme center is expected to facilitate future assignment and structural interpretation of hyperfine shifted amino acid resonances in the heme cavity. The potential utility of NOEs for resonance assignment and structure determination in large paramagnetic proteins is discussed.

Horseradish peroxidase, HRP, is a *b*-type hemoprotein consisting of a ferric heme and a single polypeptide chain.[2-4] This glycoprotein of molecular weight $\sim$42 kilodalton catalyzes the decomposition of H_2O_2 into water at the expense of organic proton donors.[2-4] This readily isolatable and extremely stable enzyme has been the subject of prolonged and comprehensive studies of both its reactivity and physical properties in its various reactive as well as nonreactive forms. The inability to obtain suitable single crystals for X-ray diffraction, however, has pressed other indirect methods[5-12] to the limit in attempting to define the structure of the enzyme, particularly with respect to the amino acid side chains in the heme pocket involved in the catalytic cycle.

Nuclear magnetic resonance presents potentially the most powerful spectroscopic method for elucidating structural features of the heme cavity.[13-16] Since HRP is a high molecular weight enzyme and paramagnetic in each of its functional states as well as in most nonfunctional derivatives, numerous modern NMR methodologies, such as the 2-D techniques,[17] are not practical. Moreover, chemical shifts for resolved resonances are dominated by hyperfine interaction from which structural information can only be obtained in certain oxidation/spin states and only if the origin of the hyperfine shifts is understood in detail. However, in favorable circumstances, the analysis of such shifts will lead to not only a detailed understanding of the electronic structure and magnetic properties of the heme center, but the shifts can be analyzed quantitatively to determine the stereochemistry of the amino acid side chain in the heme cavity. Such an analysis[18] has as its foundation the location and unambiguous assignment of all of the signals for the residues of interest, including those of the heme, the axial histidine, and the distal side chains proposed to function in the catalytic cycle, a distal histidine and an arginine.[19,20]

The single-crystal X-ray structure of another heme peroxidase, cytochrome *c* peroxidase, CcP, has been solved,[19,20] and the arginine and histidine side chains in the distal pocket are shown to be configured so as to be able to serve as the catalytic sites for reaction with H_2O_2. Although there is some homology in the polypeptide chain between CcP[21] and HRP[22] to suggest the presence of both of these side chains in the HRP distal pocket, there exists little direct evidence to support this view.

* Address all correspondence to: Professor Gerd N. La Mar, University of California, Department of Chemistry, Davis, California 95616 ((916) 752-0958).

(1) (a) Department of Chemistry. (b) UCD NMR Facility.
(2) Dunford, H. B. *Adv. Inorg. Biochem.* **1982**, *4*, 41-68.
(3) Dunford, H. B.; Stillman, J. S. *Coord. Chem. Rev.* **1976**, *19*, 187-251.
(4) Caughey, W. S. In *Inorganic Biochemistry*; Eichorn, G. L., Ed.; Elsevier: Amsterdam, 1973; Vol. 2, Chapter 24.
(5) Colvin, J. T.; Rutter, R.; Stapleton, H. J.; Hager, L. P. *Biophys. J.* **1983**, *41*, 105-108.
(6) Nozawa, T.; Kobayashi, N.; Hatano, M.; Ueda, M.; Sogami, M. *Biochim. Biophys. Acta* **1980**, *626*, 282-290.
(7) Callahan, P. M.; Babcock, G. T. *Biochemistry* **1981**, *20*, 952-958.
(8) La Mar, G. N.; de Ropp, J. S.; Smith, K. M.; Langry, K. C. *J. Biol. Chem.* **1980**, *225*, 6646-6652.
(9) La Mar, G. N.; de Ropp, J. S.; Smith, K. M.; Langry, K. C. *J. Biol. Chem.* **1981**, *256*, 237-243.
(10) de Ropp, J. S.; La Mar, G. N.; Smith, K. M.; Langry, K. C. *J. Am. Chem. Soc.* **1984**, *106*, 4438-4444.
(11) Morishima, I.; Ogawa, S.; Inubushi, T.; Yonezawa, T.; Iizuka, T. *Biochemistry* **1977**, *16*, 5109-5115.
(12) Williams, R. J. P.; Wright, P. E.; Mazza, G.; Ricard, J. R. *Biochim. Biophys. Acta* **1975**, *581*, 127-147.
(13) Wuthrich, K. *Struct. Bonding (Berlin)* **1970**, *8*, 53-121.
(14) Morrow, J. S.; Gurd, F. R. N. *CRC Crit. Rev. Biochem.* **1975**, *3*, 221-287.
(15) La Mar, G. N. In *Biological Application of Magnetic Resonance*; Shulman, R. G., Ed.; Academic: New York, 1979; pp 305-343.
(16) La Mar, G. N.; Walker, F. A. In *The Porphyrin*; Dolphin, D., Ed.; Academic: New York, 1979; Vol. 4, pp 61-157.
(17) Turner, D. L. *Prog. Nucl. Magn. Reson. Spectrosc.* **1985**, *17*, 281-358.
(18) Williams, G.; Moore, G. R.; Porteous, R.; Robinson, M. N.; Soffe, N.; Williams, R. J. P. *J. Mol. Biol.* **1985**, *183*, 409-428.
(19) Poulos, T. L.; Kraut, J. *J. Biol. Chem.* **1980**, *255*, 8199-8205.
(20) Finzel, B. C.; Poulos, T. L.; Kraut, J. *J. Biol. Chem.* **1984**, *259*, 13027-13036.
(21) Takio, K.; Titani, K.; Ericsson, L. H.; Yonetani, T. *Arch. Biochem. Biophys.* **1980**, *203*, 615-629.
(22) Welinder, K. G. *Eur. J. Biochem.* **1979**, *96*, 483-502.

0002-7863/87/1509-0265$01.50/0

We have explored the information content of ^1H NMR of the various paramagnetic forms of HRP[8-10,23] and found that, although a considerable amount of specific and useful information was obtainable from all derivatives, in no case could the data bear on the nature of the distal pocket environment. The problem in each case involved the inability to resolve and/or assign resonances. Ideally, all of the resonances of both the heme and the proximal and distal residue should be assigned. In resting-state HRP and compound I, HRP-I, the large contact shifts permitted resolution of many heme protons;[8,9] for the same reason, the nonbonded amino acid side chain experienced negligible shifts and could be neither resolved nor assigned. A similar situation holds for HRP-I.

The nonfunctional low-spin cyanide derivative, HRPCN, on the other hand, possesses considerable magnetic anisotropy[24] and hence exhibits significant dipolar shifts for amino acid side chains. The analysis of such dipolar shifts, however, first requires the determination of the magnetic axis and the relative magnitudes of the components of the susceptibility tensor.[25] The precursor to obtaining this information is the understanding of the hyperfine shifts of the heme resonances, and this requires first location and unambiguous assignment of each of the functional groups on the heme.

Our initial efforts focused on reconstitution with isotope-labeled heme and assignment of ^1H peaks based on their disappearance in the ^1H NMR spectra of specific ^2H-labeled complexes.[10] While this leads to some important assignments that allowed deduction of the orientation of the heme in the cavity, only 3 of the 22 heme signals could be assigned specifically (3-CH_3, 8-CH_3, and 4-H_α), and 6 more could be identified into collective sets (i.e., 4 vinyl H_β's and 2 propionate H_β's), leaving 13 completely undetected, largely within the intense diagmagnetic envelope. This is despite the introduction of ^2H labels into all but the four propionate α-positions.

We present herein the results of a comprehensive ^1H NMR study of HRPCN which, utilizing a combination of isotope labeling, saturation transfer spectroscopy,[26] and homonuclear Overhauser effect,[27] NOE, measurements, locate and unambiguously assign for the first time all 22 of the heme signals in a hemoprotein. The three methods to some degree provide independent assignments and hence serve as important controls for evaluating our respective approaches. For most of the signals, only the combination of methods leads to the required assignments. The methods used, however, should have general application for studying large paramagnetic heme enzymes. The resulting hyperfine shift pattern yields valuable insight into the heme electronic/magnetic properties that will facilitate future assignments of amino acid side-chain signals of interest.

Principles

Saturation Transfer. The interconversion between two forms of a protein on a time scale comparable to the intrinsic relaxation times of nuclei can lead to establishing connectivities between resonances.[26] If assignments are known in one protein form, magnetization (saturation) transfer will identify the same resonance in the other protein form. We take advantage here of the fact that the large scalar interaction leads to the resolution of most heme signals in the resting state, high-spin ferric HRP.[8] A combination of extensive isotope labeling in conjuction with NOE measurements has led to the assignment of all of the resolved heme resonances in HRP, as reported elsewhere.[28] The ligation of cyanide can be represented by reaction 1, where it has been shown[3] that $\tau_{on}^{-1} = k_2[CN^-] \sim 10^3\ s^{-1}$ and $\tau_{off}^{-1} = k_1 \sim 1\ s^{-1}$. Thus for

$$HRP + CN^- \underset{\tau_{off}^{-1}}{\overset{\tau_{on}^{-1}}{\rightleftharpoons}} HRPCN \quad (1)$$

a sample containing both HRP and HRPCN, the rate-limiting step for the interconversion between HRP and HRPCN is the first-order bond-rupture rate, k_{off}. Upon saturation of a signal in HRP (designated A), the equilibrium intensity, I, of the same signal in HRPCN (designated B) is reduced from $I_B(0)$ to $I_B(\infty)$. The two intensities are related via[29] eq 2, where T_{1B} is the intrinsic

$$\frac{I_B(\infty)}{I_B(0)} = \frac{\tau_B}{\tau_B + T_{1B}} \quad (2)$$

spin–lattice relaxation time for the signal in the B form (HRPCN) and $\tau_B = \tau_{off}$. Saturation transfer, i.e., the reduction of the related resonance in HRPCN upon saturation of a peak in HRP, will be detectable when $\tau_B \leq 10T_{1B}$.

Nuclear Overhauser Effects. The NOE, η, for a proton H_i represents the fractional intensity change of its resonance upon saturation of another resonance, H_j, in the same molecular species (i.e., solely within HRPCN). The buildup of the NOE is time dependent and for an isolated two-spin system takes the form[27] of eq 3, where $\rho_i^{-1} = T_{1i}$, the selective spin–lattice relaxation time

$$\eta_i(t) = \frac{\sigma_{ij}}{\rho_i}(1 - e^{-\rho_i t}) \quad (3)$$

of H_i, t is the duration of the saturating pulse on H_j, and σ_{ij} is the cross-relaxation rate between H_i and H_j. In the relevant high-field case ($\omega^2\tau_c^2 \gg 1$), the cross-relaxation rate is given by

$$\sigma_{ij} = \frac{-\hbar^2\gamma^4}{10r_{ij}^6}\tau_c \quad (4)$$

where τ_c is the reorientation time of the vector defined by H_i and H_j and r_{ij} is the length of this vector. For very short irradiation times

$$\eta_i(t) = \sigma_{ij}t \quad (5)$$

and hence η_i becomes independent of the intrinsic relaxation time of the nucleus. For long irradiation times, the steady state is reached:

$$\eta_i(\infty) = \sigma_{ij}/\rho_i \quad (6)$$

While NOEs have been extensively used to establish spatial proximity of pairs of nuclei in small diagmagnetic systems,[30-34] their use in large proteins[35] or paramagnetic systems[36-39] has been highly restricted because spin diffusion in large systems obscures selective primary NOEs and in the belief that efficient paramagnetic relaxation (large ρ) would render η negligible. Thus the few applications reported[36-39] have usually focused on small proteins in the low-spin, ferric state. The independence of the

(23) La Mar, G. N.; de Ropp, J. S. *J. Am. Chem. Soc.* **1982**, *104*, 5203–5206.
(24) Blumberg, W. E.; Peisach, J.; Wittenberg, B. A.; Wittenberg, J. B. *J. Biol. Chem.* **1968**, *43*, 1854–1862.
(25) Horrocks, W. D., Jr. In *NMR of Paramagnetic Molecules*; La Mar, G. N., Horrocks, W. D., Jr., Holm, R. H., Eds.; Academic: New York, 1973; pp 85–126.
(26) Keller, R. M.; Wuthrich, K. *Biol. Magn. Reson.* **1981**, *3*, 1–52.
(27) Noggle, J. H.; Shirmer, R. E. *The Nuclear Overhauser Effect*; Academic: New York, 1971.
(28) Thanabal, V.; de Ropp, J. S.; La Mar, G. N., unpublished results.
(29) Sandstrom, J. *Dynamic NMR Spectroscopy*; Academic: New York, 1982; Chapter 4.
(30) Bothner-by, A. A.; Noggle, J. H. *J. Am. Chem. Soc.* **1979**, *101*, 5152–5155.
(31) Wagner, G.; Wuthrich, K. *J. Magn. Reson.* **1979**, *33*, 675–680.
(32) Dobson, C. M.; Olejniczak, E. T.; Poulsen, F. M.; Ratcliffe, G. *J. Magn. Reson.* **1982**, *48*, 97–110.
(33) Olejniczak, E. T.; Poulsen, F. M.; Dobson, C. M. *J. Am. Chem. Soc.* **1981**, *103*, 6574–6580.
(34) Mabbutt, B. C.; Wright, P. E. *Biochim. Biophys. Acta* **1985**, *832*, 175–185.
(35) Dalvit, C.; Ho, C. *Biochemistry* **1985**, *24*, 3398–3407.
(36) Redfield, A. G.; Gupta, R. K. *Cold Spring Harbor Symp. Quant. Biol.* **1971**, *36*, 405–411.
(37) Ramaprasad, S.; Johnson, R. D.; La Mar, G. N. *J. Am. Chem. Soc.* **1984**, *106*, 5330–5335.
(38) Keller, R. M.; Wuthrich, K. *Biochim. Biophys. Acta* **1980**, *621*, 204–217.
(39) Trewhella, J.; Wright, P. E.; Appleby, C. A. *Nature (London)* **1980**, *280*, 87–88.

NOE of relaxation at short irradiation times (eq 5) dictates that NOEs should have wide applicability in paramagnetic systems if resonances can be saturated quickly. We have shown that even steady-state NOEs are readily observed in strongly paramagnetic systems, particularly for large proteins where σ is large (eq 4), allowing unambiguous assignment of heme signals not only in high-spin ferric metaquo myoglobin[40] and resting-state HRP[28,41] but also in unstable reactive intermediates such as HRP-I.[41] The paramagnetism diminishes the NOEs compared to diamagnetic systems but at the same time undermines spin diffusion[42] so that highly selective NOEs can be detected in large molecules.[28,41] The resulting NOEs therefore reflect primarily an internuclear distance of $\sim$<3 Å and hence are ideally suited for probing nearest-neighbor nuclei on the heme.

Experimental Section

Horseradish peroxidase (HRP), type VI, was purchased from Sigma as a lyophilized, salt-free powder and used directly without further purification; the protein is predominantly isozyme C. HRPCN complexes reconstituted with meso-perdeuteriated hemin (70%) and 6,7-β-$(C^2H_2)_2$ hemin (90%) used in this study are the same as those reported earlier.[10] Solutions for proton NMR studies were 3 mM in protein in 100% ^2H_2O. The solution pH, adjusted by using 0.2 M ^2HCl and 0.2 M NaO^2H, was measured with a Beckman Model 3550 pH meter equipped with an Ingold microcombination electrode; pH values are not corrected for the isotope effect. Excess solid KCN was added to the protein to generate solutions of HRPCN. For the experiments utilizing a mixture of HRP/HRPCN as described below, the appropriate fractional equivalent of cyanide was added in ^2H_2O. Typically, a mixture of HRP/HRPCN in the ratio 65:35 was used for saturation transfer among the methyls and resolved signals. Location of single-proton resonances in the crowded diamagnetic region demanded higher CN^- concentration in the mixture of HRP/HRPCN (35:65).

Saturation transfer experiments were conducted on a Nicolet NT-360 FT NMR spectrometer operating at 360.065 MHz in the quadrature mode, with 16K data points collected over a 80-kHz bandwidth. To specifically saturate a given resonance, a selective decoupler pulse of 0.2–0.4 W was used to 30 ms; the recycle time was 225 ms. Spectra were acquired in an interleaved fashion, first by saturating the resonance of interest and then by applying the decoupler significantly off-resonance for an equal time interval to create the reference file.[40] Generally, 512 scans were acquired sequentially into each interleaved data set, and the total number of scans per file was 15–20 × 10^3. Difference spectra were obtained by subtracting the transformed off-resonance spectrum from the on-resonance spectrum.

Proton NOE measurements were performed on a Nicolet NT-500 FT NMR spectrometer operating at 500.027 MHz in the quadrature mode; 8K data points were collected over a 35-kHz bandwidth. The data were collected in a similar fashion as described for the saturation transfer experiment. The time-dependent NOE spectra were collected with the decoupler pulse length varying from 4 to 300 ms; the recycle time was 0.5 s. Ninety-six scans were acquired sequentially into each interleaved data set, and the total number of scans per file was 6–7.5 × 10^3. Signal-to-noise was improved by exponential apodization which introduced 10–30-Hz line broadening. Peak shifts were referenced to the residual water signal which in turn was calibrated against internal 2,2-dimethyl-2-silapentane-5-sulfonate (DSS). Chemical shifts are reported in parts per million, ppm, with downfield shifts taken as positive. Truncated NOE data were analyzed by a three-parameter nonlinear least-squares-fit method. Nonselective T_1's were determined by a variation of the standard inversion–recovery sequence to include a composite 180° pulse. Selective T_1's were determined via eq 3 or by use of an inversion–recovery sequence employing a selective 180° decoupler pulse followed by an (hard) observation pulse. T_1 data were also analyzed via a three-parameter nonlinear least-squares fit.

Results

Assignment by Saturation Transfer. The low-field hyperfine-shifted portion of the 360-MHz ^1H NMR spectrum of a mixture of resting-state HRP and HRPCN is illustrated in trace A of Figure 2. The broad peaks in the region 30–80 ppm all arise from HRP, and the assignments of the heme signals, as determined by isotope labeling[8] and NOEs solely within the high-spin HRP,[28] are given above each peak. The low-spin HRPCN signals are narrower and are resolved in the region 10–30 ppm; assignments previously determined by isotope labeling[10] are again given above

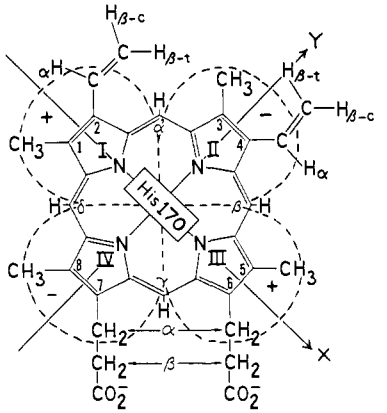

Figure 1. Structure and numbering system for hemin in HRPCN with 2,4-vinyls in the trans and cis orientations, respectively. The in-plane magnetic axes x and y are shown. The orientation of the proximal histidine is also shown along the x axis. The rhombic magnetic anisotropy as a function of cos 2Ω yields a cloverleaf-shaped distribution of dipolar shift with the lobes alternating in sign. The nodes must pass through the meso-H's (see text). The positive rhombic geometric factor along the x axis with $\chi_y > \chi_x$ yields positive rhombic shift (upfield) along the x axis as indicated by the sign of lobes.

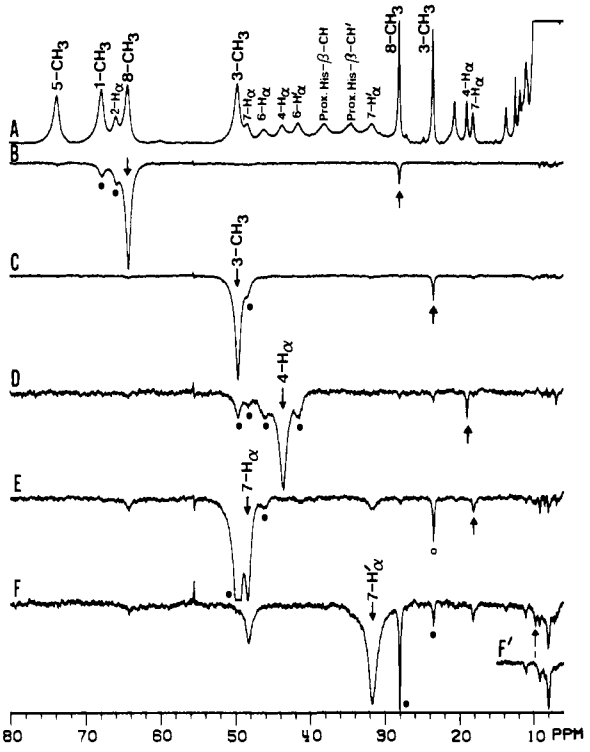

Figure 2. The hyperfine shifted portions of the 360-MHz ^1H NMR spectrum of (A) a mixture of HRP/HRPCN in the ratio 65:35 in 100% ^2H_2O at 55 °C, pH 7.0. Previously assigned resonances are labeled. B–F are the saturation transfer difference spectra generated by subtracting the reference spectrum with the decoupler off-resonance from a similar spectrum of the same sample in which the desired resonance was saturated. In each of the difference spectra B–F, a downward arrow indicates the peak being saturated and an upward arrow indicates saturation transfer. A filled circle denotes off-resonance power spillage while an open circle denotes saturation transfer from off-resonance saturation. The difference spectra B–F show the saturation of 8-CH_3, 3-CH_3, 4-H_α, 7-H_α, and 7-H'_α resonances of HRP, respectively, and the saturation transfer to their counterparts in HRPCN. The inset F′ shows the portion of the difference spectrum obtained by using the sample without CN^-; note the disappearance of the resonance at 9.74 ppm.

(40) Unger, S. W.; Lecomte, J. T. J.; La Mar, G. N. *J. Magn. Reson.* **1985**, *64*, 521–526.
(41) Thanabal, V.; de Ropp, J. S.; La Mar, G. N. *J. Am. Chem. Soc.* **1986**, *108*, 4244–4245.
(42) Kalk, A.; Berendsen, J. J. C. *J. Magn. Reson.* **1976**, *24*, 343–366.

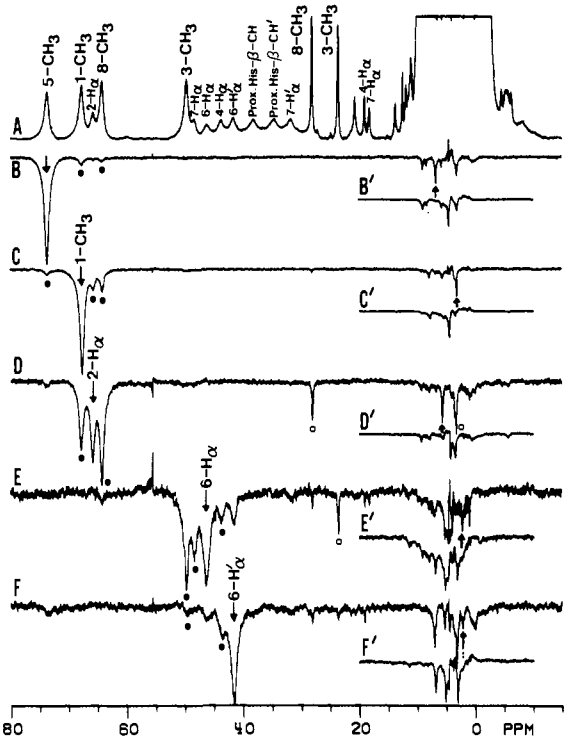

Figure 3. 360-MHz ^1H NMR spectrum of (A) a mixture of HRP/HRPCN in the ratio 65:35 in 100% ^2H_2O at 55 °C, pH 7.0. Previously assigned resonances are labeled. B–F are the saturation transfer difference spectra obtained as described in Figure 2. In each of the difference spectra B–F, a downward arrow indicates the peak being saturated and an upward arrow indicates saturation transfer. A filled circle denotes power spillage while an open circle denotes saturation transfer from off-resonance saturation. The saturation transfer involving the location of single-proton resonances in the diamagnetic region was done by using a higher concentration of CN^- to yield a mixture of HRP/HRPCN in the ratio 35:65. The difference spectra B–F show the saturation of 5-CH_3, 1-CH_3, 2-H_α, 6-H_α, and 6-H'_α resonances of HRP, respectively, and the saturation transfer to their counterparts in HRPCN. The insets B′–F′ show the portions of the NOE difference spectra obtained by employing HRP alone (without CN^-) under identical conditions. The disappearance of the peaks responsible for saturation transfer is clearly evident in all the inset spectra. The peaks upfield of the upward arrows in traces E and F are the result of poor cancellation of the intense diamagnetic resonances in that region.

the peaks. Difference spectra obtained upon saturation of the HRP signals 8-CH_3, 3-CH_3, and 4-H_α in traces B–D of Figure 2 clearly show saturation transfer to the same peak previously assigned in HRPCN by isotope labeling. For the heme 3-CH_3 and 8-CH_3, the degree of saturation transfer is ~10% under the prevailing conditions. Irradiation of 7-H_α of HRP shows saturation transfer to a resolved peak in HRPCN (Figure 2E) which was tentatively assigned[10] as 7-H_α on the basis of its titration behavior. All other low-field heme HRP signals failed to yield detectable saturation transfer to any other resolved HRPCN signal. For example, when 7-H'_α in HRP is saturated (Figure 2F), the only peak in the difference spectrum that can be associated with saturation transfer occurs at 9.74 ppm and must originate in 7-H'_α in HRPCN. The other peaks in the difference spectrum occur exclusively due to NOEs within the pure HRP complex,[28] as illustrated by the difference spectrum obtained in the absence of cyanide in the inset to Figure 2F. Saturation of the same HRP resonance with and without a small amount of cyanide present thus provides the quantitative control experiment to identify the saturation transfer connected peak in HRPCN.

The location of other unresolved HRPCN heme resonances is illustrated in Figure 3. Saturation of 5-CH_3 (Figure 3B) and 1-CH_3 (Figure 3C) of HRP yields the same peaks in HRPCN; the degree of saturation is essentially the same as for the two resolved methyls. Saturation of 2-H_α in HRP (Figure 3D) yields several peaks in the difference spectrum, but only one is missing

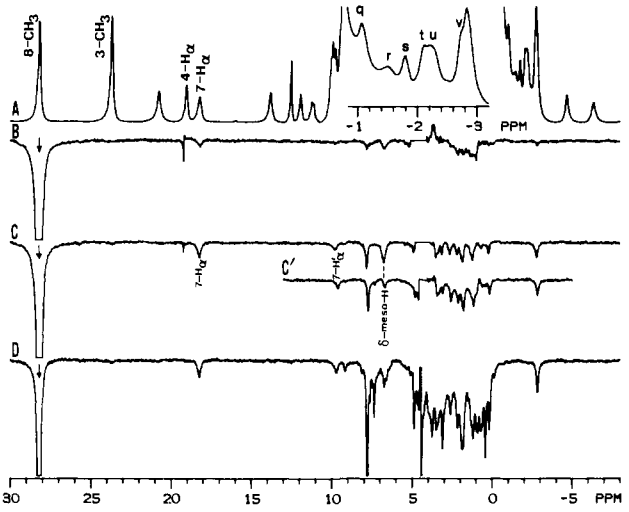

Figure 4. 500-MHz ^1H NMR spectrum of (A) 3 mM HRPCN in 100% ^2H_2O at 55 °C, pH 7.0; the inset to trace A shows the expanded section of the crowded region −1.0 to −3.0 ppm. The vinyl H_β's are collectively labeled as q, s, t, and v while the peak u represents the two-proton resonance arising from 6-H_β's.[10] Previously assigned peaks are labeled. B–D are the NOE difference spectra obtained as described in Figure 2. In each of the difference spectra B–D, a downward arrow indicates the peak being saturated. Traces B–D show saturation of the 8-CH_3 resonance for 10, 30, and 300 ms. The inset C′ shows the portion of the NOE difference spectrum obtained with meso-perdeuteriated HRPCN resulting in the disappearance of the δ-meso-H resonance.

at 5.55 ppm when the same experiment is carried out in the absence of cyanide (inset to Figure 3D). The saturation of the two 6-H_α peaks (Figure 3E,F) yields numerous peaks in the difference spectra. Comparison with the difference traces in the absence of CN (insets to Figure 3E,F) identifies the two 6-H_α peaks at 2.1 and 2.0 ppm in HRPCN. The smaller degrees of saturation (due to shorter T_1's for propionate H_α's) dictated the use of a higher CN concentration.

This exhausts the possibilities of heme signal assignments in HRPCN by saturation transfer. Thus, while two individual vinyl H_β signals have been uniquely identified in HRP,[8] their resonance positions (−2 to −5 ppm) overlap those of the known collective four vinyl H_β peaks in HRPCN,[10] precluding the saturation of the HRP peak without simultaneous saturation of the analogous HRPCN resonances. Remaining are the location of the four meso-H's and the four propionate H_β's and the individual assignment of the four vinyl H_β peaks in HRPCN.

Measurement of the T_1 for 8-CH_3 in HRPCN by selective inversion–recovery yields $T_1 \sim 40$ ms. The 10% saturation observed in conjunction with eq 2 yields a τ_{off} of ~400 ms at 55 °C.

Assignment by NOEs. The 500-MHz ^1H NMR spectrum of pure HRPCN at 55 °C is illustrated in trace A of Figure 4; the inset in the center gives the expanded section of the crowded region −1.0 to −3.0 ppm. The peaks q, s, t, and v have been shown[10] to originate collectively in the four vinyl H_β's. The peak u, which consists of two protons, was shown[10] to arise solely from propionate H_β's. Complete saturation of 8-CH_3 as a function of irradiation time yields the sequence of traces in Figure 4B–D. At short times, a significant number of peaks can be detected in the difference trace; these peaks appear to evolve monotonically with t. At longer times, several new peaks appear, and there is a general buildup of intensity in the difference spectrum in the whole diamagnetic aliphatic region, strongly indicating the development of multiple secondary NOEs or spin diffusion.[42] The lack of selectivity in NOEs appears to become serious only for irradiation times much longer than 50 ms. It may be noted that 8-CH_3 yields an NOE to the assigned 7-H_α at 18 ppm. Moreover, at 300 ms, the secondary NOE from 7-H_α to 7-H'_α at 9.74 ppm can be detected. The strong peak at 6.7 ppm in the difference spectrum in Figure 4B yields a strong temperature dependence which extrapolates to a diamagnetic shift (at $T^{-1} = 0$) of ~12 ppm (Figure 5). Such

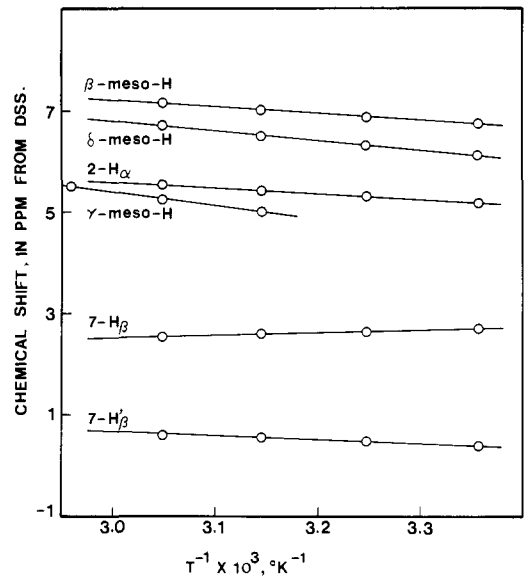

Figure 5. Curie plots of the chemical shifts vs. reciprocal temperature of the resonances in HRPCN at pH 7.0 located by NOE technique; the extrapolated diamagnetic intercept at $T^{-1} = 0$ is given in Table I.

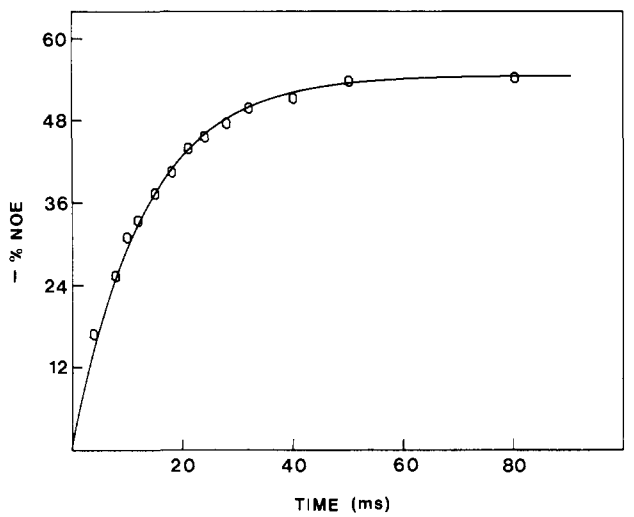

Figure 6. Plot of time-dependent buildup of the NOE to the geminal partner 7-H'$_\alpha$ at 9.65 ppm following the presaturation of 7-H$_\alpha$ for varying times from 4 to 80 ms. The solid line represents a fit of the data using eq 3 in the text. Analysis of the data yields σ(7-H$_\alpha$-7-H'$_\alpha$) = −36 Hz and ρ(7-H'$_\alpha$) = 66 Hz.

a low-field intercept is strongly indicative of a meso-H, presenting an argument for the assignment of this peak to δ-meso-H in HRPCN. The large NOE is consistent with the proximity of the methyl and meso protons. This assignment is confirmed by noting that this peak in the difference spectrum disappears when the same experiment is carried out on HRPCN reconstituted with hemin perdeuteriated at the four meso positions[10] (inset to Figure 4C). The remaining NOEs at short times must reflect NOEs to nearby amino acid resonances. It is not possible to propose any consistent assignments of amino acid resonances on the basis of the present data.

The quantitative use of NOEs and the dominance of primary NOEs at short irradiation times are strongly supported by a study of the time dependence of the NOE between 7-H$_\alpha$ at 18 ppm and its geminal partner at 9.74 ppm identified by saturation transfer. $\eta(t)$ for the 7-H'$_\alpha$ peak at 9.74 ppm upon saturation of 7-H$_\alpha$ is illustrated in Figure 6. The solid line represents the computer least-squares fit of the data points to eq 3, which yields $\sigma = -36$ Hz and $\rho = 66$ Hz. Since the propionate 7-α-CH$_2$ interproton distance is known to be 1.77 Å, eq 4 yields $\tau_c = 20$ ns for the reorientation rate of this interproton vector. This correlation time

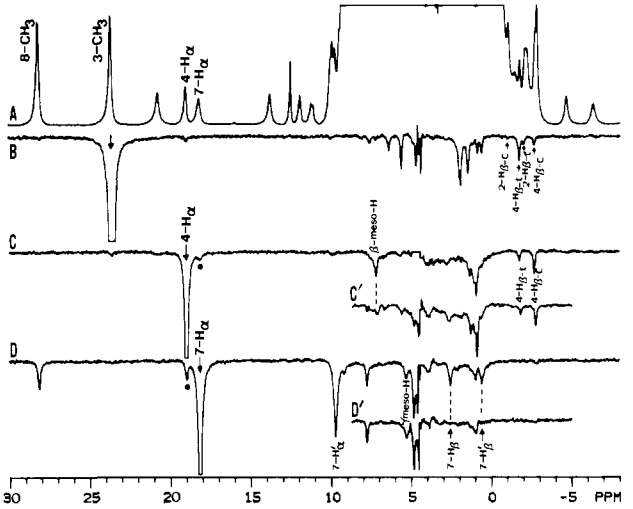

Figure 7. 500-MHz ^1H NMR spectrum of (A) 3 mM HRPCN in 100% ^2H_2O at 55 °C, pH 7.0. Previously assigned peaks are labeled. Traces B–D are the NOE difference spectra generated as described in Figure 2. In each of the difference spectra B–D, a downward arrow indicates the peak being saturated; filled circles denote effects due to power spillage. B is the saturation of 3-CH$_3$; note NOEs to all four vinyl H$_\beta$'s. (C) Saturate 4-H$_\alpha$; note NOEs to 4-H$_{\beta\text{-c}}$, 4-H$_{\beta\text{-t}}$, and β-meso-H. The inset C' shows the portion of the NOE difference spectrum obtained with meso-perdeuteriated HRPCN; note the disappearance of the β-meso-H resonance. (D) Saturate 7-H$_\alpha$; note the strong NOEs to 7-H'$_\alpha$, 7-H$_\beta$, 7-H'$_\beta$, and γ-meso-H. The inset D' shows the portion of the NOE difference spectrum obtained by using HRPCN reconstituted with 6,7-β-(C^{2}H$_2$)$_2$ hemin; note the disappearance of the 7-H$_\beta$ and 7-H'$_\beta$ resonances.

compares very well with the overall protein tumbling time at 55 °C as obtained from ^2H NMR quadrupolar relaxation of deuterium labels on the heme skeleton (20 ns).[43] Thus the NOE is primary and well-behaved in the time scale 0 to ~50 ms. All subsequent NOE experiments are restricted to a saturation time of 30 ms.

Saturation of the assigned 3-CH$_3$ yields the difference trace of Figure 7B; the peak at 1.9 ppm loses intensity upon meso-deuteriation[10] (not shown), identifying the α-meso-H signal. Interestingly, NOE connectivities are observed *to all four of the vinyl H$_\beta$'s* (see below). Trace C in Figure 7 illustrates the effect of saturating 4-H$_\alpha$; three strong NOEs are observed beside some weak composite peaks in the diamagnetic methyl region ~0.5 ppm. The two known[10] vinyl H$_\beta$ peaks s and v are thus identified with the 4-vinyl group; the geometry of the group dictates that v is 4-H$_{\beta\text{-c}}$ and s is 4-H$_{\beta\text{-t}}$. The other NOE at 7.15 ppm again yields a low-field intercept in the Curie plot (Figure 5) and is absent when using meso-deuteriated hemin (inset to Figure 7C), unambiguously establishing its origin as the β-meso-H. Saturation of the assigned 7-H$_\alpha$ peak (Figure 7D) again yields only a limited number of well-resolved peaks in the difference spectrum. Most clearly seen is the geminal partner at 9.7 ppm, 7-H'$_\alpha$. The peak at 5.25 ppm is absent when using meso-perdeuteriated hemin (not shown), and the peaks at 0.57 and 2.54 ppm are missing when the experiment is carried out on a sample reconstituted with hemin deuteriated solely at the four propionate β-positions (inset to Figure 7D). The proximity of 4-H$_\alpha$ to only β-meso-H establishes this position as the origin of the signal at 5.25 ppm. The two peaks at 0.57 and 2.54 ppm originate from the two 7-propionate H$_\beta$'s; the peak at 2.54 ppm is the more intense at very short saturation times, dictating that 7-H$_\alpha$ is closer to it than the H$_\beta$ resonating at 0.57 ppm. Since the resolved two-proton peak u has been shown to originate solely in propionate H$_\beta$'s on the basis of isotope labeling, the two contributing resonances must be the two 6-H$_\beta$ peaks.

The two remaining 2-vinyl H$_\beta$'s are assigned in Figure 8. Saturation of peak q yields a large NOE to its necessarily geminal

(43) Thanabal, V.; Johnson, R. D.; La Mar, G. N., unpublished results.

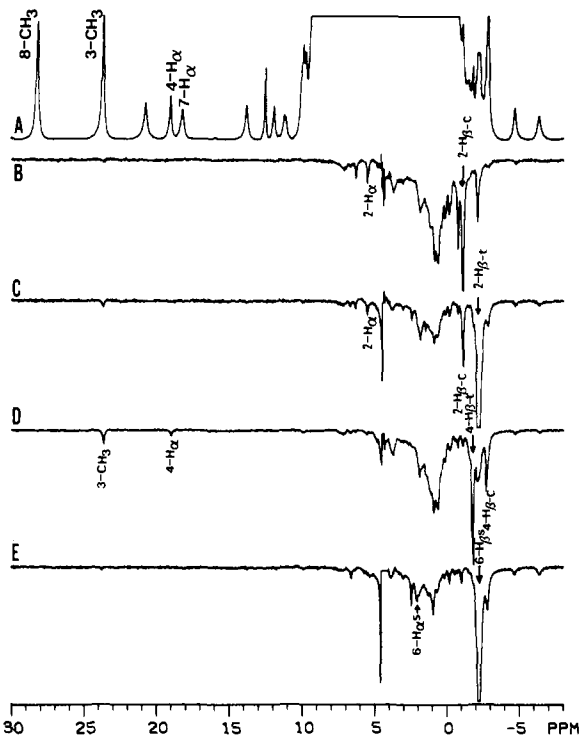

Figure 8. 500-MHz ^1H NMR spectrum of (A) 3 mM HRPCN in 100% ^2H_2O at 55 °C, pH 7.0. Previously assigned peaks are labeled. B–E are the NOE difference spectra obtained as described in Figure 2. In each of the difference spectra B–E, a downward arrow indicates the peak being saturated. The peaks in the region 0–3.0 ppm are due to the power spillage to the intense diamagnetic envelope. (B) Saturate 2-$H_{\beta\text{-c}}$; note NOEs to 2-$H_{\beta\text{-t}}$ and 2-H_α. (C) Saturate 2-$H_{\beta\text{-t}}$; note NOEs to 2-$H_{\beta\text{-c}}$ and 2-H_α. (D) Saturate 4-$H_{\beta\text{-t}}$; note NOEs to 4-$H_{\beta\text{-c}}$, 4-H_α, and 3-CH_3. (E) Saturate 6-H_β's; note NOE to peaks at 2.1 ppm.

partner, *t*; in addition a significant NOE is observed to the previously identified 2-H_α at 5.55 ppm. When t is saturated (Figure 8C), the reciprocal NOE to peak q is observed, with a much smaller NOE to 2-H_α. The geometry of the vinyl group dictates that q is 2-$H_{\beta\text{-c}}$ and t is 2-$H_{\beta\text{-t}}$. It may be noted that an NOE is observed to 3-CH_3 both when 2-$H_{\beta\text{-t}}$ (Figure 8C) as well as when 4-$H_{\beta\text{-t}}$ (Figure 8D) are saturated. The saturation of the now assigned degenerate pair of 6-H_β peaks[10] (peak u) at −2.3 ppm (Figure 8E) yields small NOEs to the pair of 6-H_α peaks at ~2.1 ppm, identified above via saturation transfer from HRP (Figure 3E,F).

The identification of unique connectivities from two different peaks to a common unresolved peak in the diamagnetic envelop (i.e., saturation transfer from 2-H_α of HRP to HRPCN (Figure 3D) and NOE from 2-H_β to 2-H_α (Figure 8B)) could be confirmed by carrying out all of the above described experiments as a function of temperature. All peaks exhibited significant temperature dependence. The resulting Curie plots for the NOE or saturation transfer located and assigned peaks in the region 0–10 ppm are illustrated in Figure 5 in the usual format of observed shift vs. reciprocal temperature.

As indicated above and illustrated in Figure 7B, saturation of 3-CH_3 in HRPCN yields NOEs to all four vinyl H_α's. A plot of the NOE buildup of the individual assigned vinyl H_β peaks as a function of saturation time of the 3-CH_3 signal is illustrated in Figure 9. The NOEs appear linearly at very short saturation times and extrapolate to the origin, indicating that all are primary NOEs.[31] The chemical shifts, referenced to DSS, of all 22 heme signals at 55 and 35 °C are listed in Table I; also included are the apparent intercepts at $T^{-1} = 0$ obtained from the Curie plots in Figure 5.

Discussion

Assignments. The location and identification of all of the 22 resonances of the heme provide the only complete assignment of

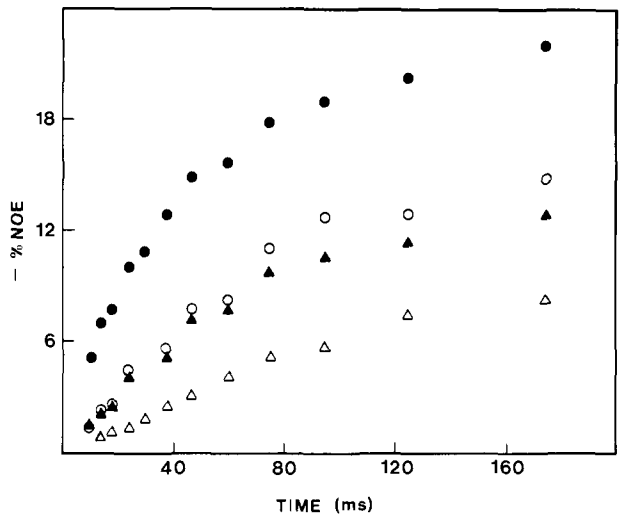

Figure 9. Plots of the time-dependent buildup of NOEs to 2-$H_{\beta\text{-c}}$ (△), 2-$H_{\beta\text{-t}}$ (▲), 4-$H_{\beta\text{-c}}$ (○), and 4-$H_{\beta\text{-t}}$ (●) as a function of the presaturation of 3-CH_3 for varying times from 10 to 175 ms. Note that the NOE buildup is linear at short irradiation times for all four peaks and extrapolates to the origin, indicating that all are primary NOEs.

Table I. Chemical Shifts[a] in ppm for All the Heme Resonances in HRPCN at pH 7.0

assignment	shifts 35 °C	shifts 55 °C	intercept at $T^{-1} = 0$ (ppm)
1-CH_3	2.85	3.05	6.40
2-H_α	5.32	5.55	9.25
2-$H_{\beta\text{-c}}$	−1.55	−1.12	5.85
2-$H_{\beta\text{-t}}$	−2.69	−2.16	6.60
α-meso-H[b]		1.9	
3-CH_3	25.07	23.65	−1.00
4-H_α	19.67	18.96	7.60
4-$H_{\beta\text{-c}}$	−3.26	−2.80	5.50
4-$H_{\beta\text{-t}}$	−2.22	−1.83	4.40
β-meso-H	6.87	7.15	11.10
5-CH_3	6.43	6.68	10.80
6-H_α		2.10	
6-H'_α		2.00	
6-H_β } [c]			
6-H'_β }	−2.79	−2.30	5.40
γ-meso-H[d]		5.25	13.25
7-H_α	19.02	18.20	5.70
7-H'_α	9.65	9.74	9.00
7-H_β	2.63	2.54	0.70
7-H'_β	0.47	0.57	3.00
8-CH_3	29.91	28.15	−0.80
δ-meso-H	6.32	6.70	12.35

[a] Chemical shifts are referenced to DSS through the residual water signal; uncertainty in shifts is ±0.02 ppm. [b] Overlaps another intense NOE in difference spectrum. [c] Both the 6-H_β's resonate at the same chemical shift. [d] γ-meso-H resonance is not resolved outside the HOD signal at a temperature below 40 °C. The variable-temperature data were collected at temperatures of 45, 55, and 65 °C.

the heme resonance of any hemoprotein to date. The location of the four meso-H signals in the range 1.9–7.1 ppm is consistent with our observation of a single meso-^2H resonance for all four meso deuterons with a chemical shift of 5.0 ± 3 ppm in the ^2H NMR spectrum of meso-$^2H_4$ hemin reconstituted HRPCN.[43]

The saturation transfer technique[26] cannot be considered a general method, since ligand exchange must occur within a narrow range of lifetimes and assignments in one form must be independently available. This method is most advantageously used in connecting high-spin and low-spin forms, such as in the present case, where the prime advantage is that all of the propionate and vinyl H_α resonances are resolved and assignable though methyl deuteriation and NOEs solely within the high-spin complex.

The use of the NOEs is more general, particularly when employed with selective isotope labeling. In HRPCN, all resonance assignments except for 5-CH_3 could have been achieved solely

on the basis of the present NOEs and the previously reported isotope-labeled derivatives. The three methods utilized simultaneously, however, provide important cross checks that establish the validity of the NOE method in the present case.

The success of the assignments in HRPCN, together with our more limited success in high-spin HRP,[28,41] indicates that paramagnetism does not interfere with detection of sizeable NOEs and, at the same time, appears to undermine spin diffusion from the heme to the protein matrix. Therefore it can be expected that comprehensive resonance assignments based on a combination of NOEs and isotope labeling should be attainable for ferric enzymes of comparable size, such as cytochrome *c* peroxidase,[44] chloroperoxidase,[45] and, most importantly, cytochrome P450.[46] In view of the fact that cross-relaxation will only increase in larger proteins such as lactoperoxidase[47] and catatase,[48] NOEs should also prove fruitful for effecting needed resonance assignments.

The measurement of the selective T_1 for the 8-CH_3 in HRPCN, in conjunction with the observation of a 10% intensity decrease upon saturation of the 8-CH_3 in HRP in equilibrium with HRPCN, leads to $\tau_{off}^{-1} = k_1 \sim 2.5\ s^{-1}$. This value is consistent with an estimate of τ_{off}^{-1} determined from the known value of $K_{eq} \sim 2 \times 10^{-6}$ M and the on-rate, $k_{on} \sim 1 \times 10^5\ M^{-1}\ s^{-1}$.

The determination of a correlation time for the α-CH_2 interproton vector reorientation that is consistent with the overall tumbling time of the protein dictates that the propionate side chain is immobile in the heme pocket. Similar constraints on side-chain mobility of the vinyl groups have been detected[43,49] by both ^1H and ^2H NMR. The quantitative fit of $\eta(t)$ to eq 3 also dictates that the two-spin approximation is valid and that spin diffusion[42] contributes insignificantly to the NOE difference spectra for irradiation times < 50 ms. This suggests that time-dependent NOEs may be profitably used to characterize internal motion of side chains of relatively large molecular weight paramagnetic enzymes.

It may be noted that the variable-temperature data obtained from NOE difference traces can also be used effectively to aid in assignments. Thus the peaks assigned to meso-H's or 2-H_α by NOEs (and confirmed by saturation transfer or deuteriation) in each case yield intercepts to the low field of this resonance position, as could be expected solely for the meso-H's and vinyl H_α's of the heme. While this method is not foolproof, such variable-temperature data can serve as a useful guide to assignments.

Vinyl and Propionate Side-Chain Orientation. The similarity of the hyperfine shifts for the two 6-propionate H_α's dictates that the heme edge-on projection of the C_α–C_β vector is essentially perpendicular to the heme plane. For the 7-propionate group, on the other hand, 7-H_α exhibits a much larger contact shift than 7-H'_α; the $\cos^2\phi$ dependence (ϕ is the dihedral angle between the heme plane normal and the C–C_α–H plane) of the shift,[50] in conjunction with the larger NOE for 8-CH_3 to 7-H_α than to 7-H'_α, dictates that the C_α–C_β vector is tilted and points toward 8-CH_3 and away from the γ-meso position. Toward which side of the heme the carboxylates are oriented cannot be determined at this time.

The pattern of NOEs from 4-H_α → β-meso-H (Figure 7C) and 4-$H_{\beta\text{-t}}$ → 3-CH_3 (Figure 8D) and the complete absence of a NOE 4-H_α → 3-CH_3 (Figure 7C) dictate that the 4-vinyl group is close to in-plane and is oriented in the cis position,[41] as depicted in Figure 1. A trans orientation for the 2-vinyl group is indicated by the absence of a detectable NOE, 2-$H_{\beta\text{-t}}$ → 1-CH_3 (Figure 8C). More direct evidence for both of these vinyl orientations is obtained from simply saturating the 3-CH_3 resonance. As shown in Figure 3C, NOEs are detected to all four vinyl H_β's. A plot of the magnitude of the NOEs for the four assigned vinyl H_α's as a function of irradiation time is illustrated in Figure 9. The appearance of all four H_β signals at the shortest irradiation times provides direct evidence that all of the NOEs are primary. Then relative magnitudes of the NOEs, 4-$H_{\beta\text{-t}}$ > 4-$H_{\beta\text{-c}}$ ≈ 2-$H_{\beta\text{-t}}$ > 2-$H_{\beta\text{-c}}$, are qualitatively consistent with distances estimated for *trans*-2-vinyl and *cis*-4-vinyl (Figure 1). The strong dipolar coupling between the two pairs of H_β's on each vinyl group renders the use of eq 3 to obtain σ invalid. The pattern of the NOEs from 3-CH_3, however, unambiguously establishes the trans and cis orientations of the 2- and 4-vinyl groups, respectively, in HRPCN. The same orientations have been proposed on the basis of ^1H NMR for both resting-state HRP and compound I[41] but are in contrast to cis orientations in reduced HRP deduced from resonance Raman interpretation.[51] The near in-plane orientation of both vinyl groups directly supports earlier proposals[49] for strong steric clamping of the heme periphery by protein contacts.

Electronic/Magnetic Properties of the Heme. Extensive ^1H NMR studies of low-spin ferric model complexes[16] have indicated that the heme hyperfine shifts arise from a combination of contact shifts from π spin delocalization and dipolar shifts due to significant magnetic anisotropy. This dipolar shift is given by eq 7, where r is the length of the Fe–H vector, θ the angle between

$$\left(\frac{\Delta H}{H}\right)_{dip} = -\frac{1}{3N}\left(\chi_z - \frac{1}{2}(\chi_x + \chi_y)\right)\frac{3\cos^2\theta - 1}{r^3} - \frac{1}{2N}[\chi_x - \chi_y]\frac{\sin^2\theta\cos 2\Omega}{r^3} \quad (7)$$

r and the z axis, and Ω the angle between the projection of r on the heme plane and the x axis; χ_x, χ_y, and χ_z are the principal components of the susceptibility tensor in the coordinate system defined in Figure 1. In the essentially axially symmetric model complexes, the pyrrole substituents exhibited dominantly contact shifts due to spin delocalization into the e_3 π molecular orbital of the heme.[16] The meso-H's, on the other hand, exhibited primarily axial dipolar shifts since the π spin density is negligible at these positions.[16] The axial dipolar shifts (first term in eq 7) are upfield for heme substituents, since $3\cos^2\theta - 1$ is negative and $\chi_z > \chi_x$ and χ_y and has been estimated at ~6 ppm for meso-H's. In proteins, low-spin ferric hemes exhibit additionally a significant in-plane anisotropy, such that the second term in eq 7 must be included in any analysis. However, while the heme normal can be assumed to correspond to the z axis, the location of the in-plane magnetic axis is not known for HRPCN.

Surprisingly, the four meso-H hyperfine shifts are very similar at 8.6–3.4 ppm (due to observed shifts of 7.1–1.9 ppm from DSS and a diamagnetic origin of 10.5 ppm from DSS). Such similar meso-H shifts dictate that either the rhombic magnetic anisotropy is small (i.e., $\chi_x \sim \chi_y$) or the magnetic axes fall along the two N–Fe–N vectors. This conclusion follows from the fact that the angular term in Ω in eq 7 changes sign every 90° and hence predicts that significant rhombic dipolar shifts must cause the two pairs of opposite meso-H's (α-H, γ-H; β-H, δ-H) to shift in opposite directions. Since there is no systematic difference in the α,γ-meso-H and β,δ-meso-H shifts and the system possesses in-plane anisotropy,[24] the magnetic axes must be as depicted in Figure 1. The relative magnitude of the rhombic geometric factor as a function of Ω yields a cloverleaf, as shown in Figure 1. For the magnetic axes as shown, the meso-H's all fall on the nodes. Since the rhombic geometric factor is positive for $\Omega = 0$, the sign of the dipolar shift depends on the relative magnitude of χ_x and χ_y, with the positive lobes of the cloverleaf along the x axis if $\chi_x < \chi_y$. The relative magnitudes of χ_x and χ_y can be unambiguously determined

(44) Satterlee, J. D.; Erman, J. E.; La Mar, G. N.; Smith, K. M.; Langry, K. C. *J. Am. Chem. Soc.* **1983**, *105*, 2099–2104.
(45) Goff, H. M.; Gonzalez-Vergara, E.; Bird, M. R. *Biochemistry* **1985**, *24*, 1007–1013.
(46) Keller, R. M.; Wuthrich, K.; Debrunner, P. G. *Proc. Natl. Acad. Sci. U.S.A.* **1972**, *69*, 2073–2075.
(47) Goff, H. M.; Gonzalez-Vergara, E.; Ales, D. C. *Biochem. Biophys. Res. Commun.* **1985**, *133*, 794–799.
(48) Morishima, I.; Ogawa, S. In *Oxidases and Related Redox Systems*; King, T. E., Mason, H. S., Morrison, M., Eds.; Pergamon: Oxford, 1982; pp 597–617.
(49) La Mar, G. N.; de Ropp, J. S.; Smith, K. M.; Langry, K. C. *J. Am. Chem. Soc.* **1983**, *105*, 4576–4580.
(50) La Mar, G. N. In *NMR of Paramagnetic Molecules*; La Mar, G. N., Horrocks, W. D., Jr., Holm, R. H., Eds.; Academic: New York, 1973; pp 85–126.
(51) Desbois, A.; Mazza, G.; Stetzkowski, K.; Lurtz, M. *Biochim. Biophys. Acta* **1984**, *785*, 161–176.

from the nature of the lone spin-containing d orbital.

The fact that the pyrrole substituent shifts exhibit primarily π contact shifts is evidenced by the similar magnitude of the downfield methyl and upfield pyrrole H shifts in deuterohemin reconstituted HRPCN[10] as well as by the downfield 4-H_α and upfield 4-H_β shifts in HRPCN.[10] The large asymmetry in the hyperfine shifts among the four pyrroles, however, is considerably greater than could conceivably arise from only rhombic dipolar shifts and arises from the fact that the spin-containing d orbital in HRPCN is primarily d_{yz} in character.[10] This predominantly d_{yz} can interact with the π orbitals of only pyrroles II and IV. Thus the increase in π contact shifts for two pyrroles and the decrease in the shifts for the other two pyrroles, as compared to a model complex, is observed in every low-spin cyanide derivative of a ferric hemoprotein and has been proposed to arise from π bonding with the axial histidyl imidazole, as discussed previously.[52,53] In HRPCN, this indicates that the axial imidazole plane is in the xz plane, as depicted schematically in Figure 1. In order that the spin-containing d orbital be primarily d_{yz}, this orbital must be higher in energy than d_{xz} and hence dictates that $\chi_y > \chi_x$.[54,55]

Thus our analysis dictates that amino acid residues located anywhere above or below pyrroles I and III should experience downfield axial and upfield rhombic shifts. Both the axial and rhombic terms yield downfield dipolar shifts for the amino acid residues over the pyrroles II and IV. Since noncoordinated amino acid can experience solely dipolar shifts, strongly upfield-shifted non-heme rsonances must arise from amino acid residues over pyrroles I and III.

This information on the expected direction of dipolar shifts for amino acids in the heme cavity, together with comprehensive NOE and variable-temperature studies of the remaining resolved resonance of HRPCN, should provide additional insight into the stereochemistry of the heme pocket of HRPCN. Such studies are in progress.

Acknowledgment. We are indebted to K. M. Smith for making available the two deuteriated hemins to confirm our assignments. This research was supported by grants from the National Institutes of Health, GM-26226, and the National Science Foundation, CHE-84-15329.

(52) Shulman, R. G.; Glarum, S. H.; Karplus, M. *J. Mol. Biol.* **1971**, *57*, 93-115.
(53) Traylor, T. G.; Berzinis, A. P. *J. Am. Chem. Soc.* **1980**, *102*, 2844-2846.
(54) Palmer, G. In *The Porphyrins*; Dolphin, D., Ed.; Academic: New York, 1979; Vol. 4, pp 313-353.
(55) Byrn, M. P.; Katz, B. A.; Keder, N. L.; Leven, K. R.; Magurany, C. J.; Miller, K. M.; Pritt, J. W.; Strouse, C. E. *J. Am. Chem. Soc.* **1983**, *105*, 4916-4922.

Communications to the Editor

First Demonstration of Solvolytic Generation of a Simple Silicenium Ion (R_3Si^+).† Access via 1,2-Methyl Migration[1]

Yitzhak Apeloig* and Amnon Stanger

Department of Chemistry, Technion—Israel Institute of Technology, Haifa 32000, Israel

Received June 12, 1986

Carbenium ions are well-established reactive intermediates and their properties have been extensively studied.[2] In contrast, numerous attempts to generate in solution the isoelectronic silicenium ions (R_3Si^+) were unsuccessful.[3] Effective methods for the generation of carbenium ions[2] have repeatedly failed when applied to the analogous organosilicon precursors.[3] Progress was achieved only recently; Lambert et al.[4a] reported the preparation of two persistent silicenium ions (i.e., $(i\text{-PrS})_3Si^+$ and Ph_3Si^+) and Eaborn et al.[4b] provided evidence for the intermediacy of bridged delocalized silicon-containing cations in the solvolysis of a special group of highly sterically congested precursors. However, to the best of our knowledge, clear evidence for the solvolytic generation of a simple tricoordinated silicenium ion has not yet been presented.[3,4] We now present strong evidence that this elusive reactive intermediate (**2**) can be generated via a 1,2-methyl migration of a solvolytically produced α-silyl carbenium ion **1** (eq 1). We note

$$R_3SiCR'_2X \xrightarrow[-X^-]{\text{solvolysis}} \underset{\mathbf{1}}{R_3SiCR'_2} \xrightarrow{\sim R} \underset{\mathbf{2}}{R_2SiCR'_2R} \rightarrow \text{products} \quad (1)$$

that similar processes, e.g., the $AlCl_3$-induced methyl migration from silicon to carbon, have been known since 1947.[5a] However, the general consensus[3,5b,c] has been that silicenium ions are not involved in these and other similar[5c] processes, believed to proceed via a four-centered transition state (or intermediate),[5b,c] but Barton et al.[5d] have recently challenged this conclusion.

Our starting point was theoretical. Ab initio calculations[6a] predict that α-silyl carbenium ions **1** are generally less stable than the isomeric silicenium ions **2**. For example, at 3-21G[6b] $(CH_3)_3SiC^+(CH_3)_2$ is 9.7 kcal·mol^{-1} less stable than $(CH_3)_2Si^+C(CH_3)_3$ and $CH_3C^+HSiH(CH_3)_2$ is less stable than $(CH_3)_2CHSi^+(CH_3)_2$ by 23.2 kcal·mol^{-1}. Furthermore, starting from **1** the calculated barriers for a 1,2-methyl shift are small, only a few kilocalories per mole.[7] Recent gas-phase experiments support these predictions. Thus, a MS/MS experiment shows that $(CH_3)_3SiCH(CH_3)Cl$ and $(CH_3)_2CHSi(CH_3)_2Cl$ produce

† These species have also been named silylenium or silacenium ions.
(1) Reported in part at the Fourth European Symposium on Organic Chemistry (ESOC), Aix-en-Provence, France, Sept 2-6, 1985, and the VIII IUPAC Conference on Physical Organic Chemistry, Tokyo, Japan, Aug 24-29, 1986.
(2) *Carbonium Ions*; Olah, G. A., Schleyer, P. v. R., Eds.; Wiley-Interscience New York, 1976.
(3) (a) Review: Corriu, R. J. P.; Henner, M. *J. Organomet. Chem.* **1974**, *74*, 1. (b) Bickart, P.; Llort, F. M.; Mislow, K. *Ibid.* **1976**, *116*, C1. (c) Cowley, A. H.; Cushner, M. C.; Riley, P. E. *J. Am. Chem. Soc.* **1980**, *102*, 624 and references therein.
(4) (a) Lambert, J. B.; Schulz, W. J., Jr., *J. Am. Chem. Soc.* **1983** *105*, 1671. Lambert, J. B.; McConnell, J. A.; Schulz, W. J., Jr. *Ibid.* **1986**, *108*, 2482. (b) Eaborn, C.; Lickiss, P. D.; Najim, S. T.; Romanelli, M. N. *J. Chem. Soc., Chem. Commun.* **1985**, 1754 and earlier work referenced therein.
(5) (a) Whitmore, F. C.; Sommer, L. H.; Gold, J. *J. Am. Chem. Soc.* **1947**, *69*, 1976. (b) Bott, R. W.; Eaborn, C.; Rushton, B. M. *J. Organomet. Chem.* **1965**, *3*, 455. (c) Brook, A. G.; Bassindale, A. R. In *Rearrangements in Ground and Excited States*; De-Mayo, P., Ed.; Academic: New York, 1980; Vol. II. (d) Robinson, L. R; Burns, G. T.; Barton, T. J. *J. Am. Chem. Soc.* **1985**, *107*, 3935.
(6) (a) A slightly modified version of Gaussian 80 was used: Binkley, J. S.; Whiteside, R. A.; Krishnan, R.; Seeger, R.; DeFrees, D. J.; Schlegel, H. B.; Topiol, S.; Kahn, L. R.; Pople, J. A. *QCPE* **1980**, *13*, 4046. (b) First row: Binkley, J. S.; Pople, J. A.; Hehre, W. J. *J. Am. Chem. Soc.* **1980**, *102*, 939. Second row: Gordon, M. S.; Binkley, J. S.; Pople, J. A.; Pietro, W. J.; Hehre, W. J. *Ibid.* **1982**, *104*, 2797.
(7) For example, in the rearrangement of $CH_3C^+HSiH(CH_3)_2$ to $(CH_3)_2CHSi^+H(CH_3)$ we estimate that the barrier for a methyl shift is only 2-3 kcal·mol^{-1}. This estimation is based on 6-31G* calculations corrected for the effect of correlation energy using the "additivity approximation" (see: Bouma, W. J.; Nobes, R. H.; Radom, L. *J. Am. Chem. Soc.* **1983**, *105*, 1743) and an MP3/6-31G* calculations for analogous smaller systems.

0002-7863/87/1509-0272$01.50/0